

Coordination diversity of *N*-phosphoryl-*N'*-phenylthiourea (LH) towards Co^{II}, Ni^{II} and Pd^{II} cations: Crystal structure of ML₂-*N,S* and ML₂-*O,S* chelates

Felix D. Sokolov^a, Nail G. Zabirov^a, Luiza N. Yamalieva^a, Valery G. Shtyrilin^a, Ruslan R. Garipov^a, Vasily V. Brusko^a, Alexander Yu. Verat^a, Sergey V. Baranov^a, Piotr Mlynarz^{b,1}, Tadeusz Glowiak^b, Henryk Kozlowski^{b,*}

^a Kazan State University, Department of Chemistry, Kremlevskaya Street 18, Kazan 420008, Russia

^b University of Wrocław, Faculty of Chemistry, F. Joliot-Curie 14, 50-383 Wrocław, Poland

Received 27 September 2005; received in revised form 2 January 2006; accepted 15 January 2006

Available online 28 February 2006

Abstract

Thiourea, PhNHC(S)NHP(O)(OPr^{*i*})₂ (LH) chelates of Co^{II}, Ni^{II}, and Pd^{II} ions have been obtained and investigated by single-crystal X-ray diffraction, UV, IR, NMR spectroscopy, and EI mass-spectrometry. The unusual 1,3-*N,S*-coordination via sulfur and NP(O) nitrogen atoms has been found in the *trans*-square-planar NiL₂ and PdL₂ complexes, whereas the 1,5-*O,S*-coordination is realized in the tetrahedral CoL₂ complex. DFT calculations have revealed significant stabilization of the 1,3-*N,S*-structures due to stronger crystal field and the NH–O=P hydrogen bonds.

© 2006 Elsevier B.V. All rights reserved.

Keywords: Thiourea coordination; Substituent effects; Co^{II} complexes; Ni^{II} complexes; Pd^{II} complexes; *N,S*-coordination; *O,S*-coordination

1. Introduction

β -Dicarbonyl compounds (*N*-acylureas **1**, acetylacetonates, etc.) and their phosphorus containing analogs (*N*-acylamidophosphinates **2**, imidodiphosphinates **3**) (Fig. 1) were found to be very attractive ligands for variety of metal ions [1–4].

β -Bifunctional ligands **1–3** contain three potential donor centers: X, Y and internal nitrogen atoms. Nucleophilic ability of the latter donor is significantly reduced by the two neighboring electron-withdrawing groups. That is why the alkylation of *N*-thioacylamido(thio)phosphates-

RC(S)NHP(Y)(OR')₂ (Y = O,S) always proceeds on the thiocarbonyl sulfur atom [1a,5].

There is a fair amount of the data concerning the structures of complexes of divalent transition metal ions of Ib, IIb, VIIIb groups with *N*-thioacylamidothiophosphinates (**2**) (X, Y = S) [1–5,7–10]. The 1,5-bidentate coordination of deprotonated ligands through sulfur atoms takes place in all these cases.

The substituents (or other factors) are hardly capable of changing a coordination mode in the complexes of *dithio*-derivatives of **2** with divalent cations of VIIIb group. Due to the strong π -interactions, the formation of metal–sulfur bonds is most energetically favorable in all these cases.

Replacement of one sulfur atom in conjugated [RC(X)NP(Y)R'₂]⁽⁻⁾ moiety to oxygen (X = S, Y = O or X = O, Y = S) leads to appearance of the ambivalent coordination modes and possible competition between the three donor centers in the binding anion species. As a result, the

* Corresponding author.

E-mail addresses: felix.sokolov@ksu.ru (F.D. Sokolov), henrykoz@wchuwr.chem.uni.wroc.pl (H. Kozlowski).

¹ Present address: Wrocław University of Technology, Wybrzeże Wyspińskiego 27, 50-370 Wrocław, Poland.

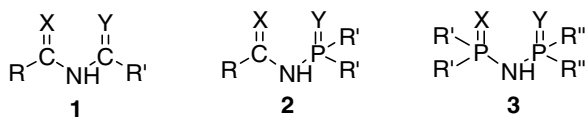


Fig. 1. Schematic representation of the structures 1–3 (X, Y = O, S).

formation of the chelate isomers with 1,3-X, N (or 1,3-Y, N) and 1,5-X,Y coordination becomes possible. This ambivalent ligand behavior was practically not investigated for compounds **2**, neither for their analogs **1** and **3**.

The numerous complexes of *N*-acylthiourea (**1**), $M[R_2NC(S)NC(O)Ar]_2$ ($I = Ni^{II}, Pt^{II}, Pd^{II}$) [11] were described; however, according to the X-ray data all of them have shown the same square planar MO_2S_2 -coordination pattern.

Much less data are available for the coordination ability of mixed-chalcogen ligands **2**. The studied complexes, $Pd[PhC(O)NP(S)Ph_2]_2$ [2], $Cu(PPh_3)[PhC(O)NP(S)Ph_2]$ [2], and $M[PhC(S)NP(O)(OPr^i)_2]_2$ ($M = Pd^{II}$ [12], Cu^{II} [13], Hg^{II} [10], and Pb^{II} [14]), exist as the 1,5-*O,S*-isomers.

N-thioacylamidothiophosphinate (**2**) complexes with the $Co^{II}O_2S_2$ [15] and $Ni^{II}O_2S_2$ [16] nuclei show a tendency to increase the coordination number around the metal ion. Two types of complexes were formed by the reaction of thioamide $PhC(S)NHP(O)(OPr^i)_2$ (HQ) potassium salt with Co(II) nitrate: the blue complex CoQ_2 with tetrahedral CoO_2S_2 core and yellow $Co(HQ)_2Q_2$ complex with square-bipyramidal $Co(O^{eq})_2(O^{ax})_2S_2$ core [15]. A square-bipyramidal $Co(O^{eq})_2(O^{ax})_2S_2$ moiety was formed by two 1,5-*O,S*-coordinating ligands in the equatorial plane and two neutral HQ molecules coordinated through phosphoryl oxygen atoms in the axial positions. The reaction of this ligand with Ni(II) nitrate resulted in the square-bipyramidal $Ni(HQ)_2Q_2$ complex [16].

The studies of the complexes of VIIIb group with imidodiphosphinates (**3**), containing non-equivalent donor atoms X and Y, were reported recently. The ligands $[Ph_2P(O)NP(Y)Ph_2]^-$ ($Y = S, Se$) coordinate to Pd^{II} ion by oxygen and Y atoms, giving the six-membered chelate rings [17]. Ni(II) also forms complexes with the mixed-chalcogen imidodiphosphinates, $Ni[Ph_2P(O)NP(S)R_2^2-O,S]_2$ ($R^2 = Ph, Me$) [18]. The latter complexes unusually have the tetrahedral NiO_2S_2 coordination core.

Presently, only five reliably known examples of the nitrogen atom involvement in the coordination with VIIIb-group metal ions for ligands 1–3 are known. These are Pd^{II} complexes with imidodiphosphinate $(PhO)_2P(O)NHP(S)R_2^2$ with $R^2 = OPh$ [19], Ph [20], *i*-Pr [20], and bis-thiophosphinate urea $[Ph_2P(S)NH]_2CO$ [21]. The structures of these complexes were solved by X-ray as **4** and **5**, which is depicted in Fig. 2.

Strong p- π conjugation in $-C(S)-N-C(O)-$ anion in combination with electron-withdrawing properties of $C=X$ groups lowers the electron density on the nitrogen, making it unlikely to be involved in the metal ion binding. However, 1,3-*N,S*-coordination was recently found in the *trans*-

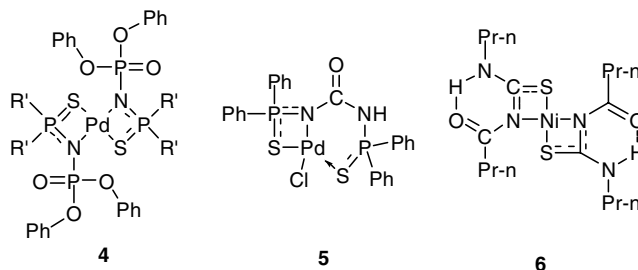


Fig. 2. Coordination modes in complexes **4**, **5** and **6**.

square-planar complex $Ni^{II}[PrC(O)NC(S)NHP^{r^i}-N,S]_2$ (**6**) [22].

As the possible reasons for the 1,3-*S,N*-chelate formation, the acceptor property of PhO at $P(O)(OPh)_2$ groups [20] and the stabilizing effect of the intramolecular hydrogen bonds [22] were suggested. However, attempts to estimate the mutual stability of the appropriate 1,3-*N,S*- and 1,5-*O,S*-species and the importance of the different stabilizing structural factors were not discussed.

Here, we report the first example of competitions between 1,3-*N,S*- and 1,5-*O,S*-coordination of thiourea $PhNHC(S)NHP(O)(OPr^i)_2$ (**LH**) in ML_2 chelates for $M = Co^{II}$ (**7**), Ni^{II} (**8**) and Pd^{II} (**9**).

2. Experimental

2.1. General information

Commercially available compounds $M(NO_3)_2 \cdot 6H_2O$ ($M = Ni, Co$) and $Pd(PhCN)_2Cl_2$ were used as supplied.

Infrared spectra were recorded in the range of 250–4000 cm^{-1} on a Specord M-80 spectrometer. Electronic absorption spectra were recorded with a Perkin–Elmer Lambda 35 spectrophotometer in $CDCl_3$ solutions in the 10^{-2} M up to 10^{-6} M concentration range of the ligand. The NMR 1H (300 MHz), ^{31}P (122.4 MHz) and ^{13}C (75.4 MHz) spectra were obtained using a Varian Unity-300 NMR spectrometer. The ^{31}P chemical shifts were calibrated indirectly to the 85% H_3PO_4 peak (δ 0.0 ppm). Mass-spectra were obtained on a TRACE MS “Finnigan MAT” instrument. Electron ionization energy was 70 eV. The substance was injected directly into the ion source at 150 °C. Heating of vaporizer-ampoule of the direct injection energy was carried out in programmed mode from 35 to 200 °C with a speed of 35 °C per minute. $M\pm$ electro-spray ionization mass-spectra were recorded on Thermo Finnigan LCQ mass-spectrometer for 10^{-6} M solution in $CHCl_3/MeOH$ mixture (1:1 v/v), speed of a sample submission was 3 $\mu L/min$, ionizing voltage was 4.10 kV, and capillary temperature was 210 °C.

2.2. X-ray crystallography

X-ray data were collected on a KUMA KM-4 diffractometer with graphite-monochromated Cu $K\alpha$ radiation using the ω - 2θ technique at 100 K. Corrections were made

for Lorentz-polarization and adsorption effect. There was no crystal decay as measured by three standard reflections. The structure was solved by direct methods (SHELXS-97) and refined by full-matrix least-squares (SHELXL-97) anisotropically for all non-hydrogen atoms [23,24]. All figures were made using the program PLATON [25]. Crystal data are summarized in Table 1.

2.3. Ligand preparation

N-diisopropoxyphosphinyl-*N'*-phenylthiourea (LH) was prepared according to the established literature method [26]. M.p. 124 °C (from CH₂Cl₂ + C₆H₁₄ 1:5) (Lit. [26], 124–125 °C from hexane). *Anal.* Calc. for C₁₃H₂₁N₂O₃PS: C, 49.36; H, 6.69; N, 8.86. Found C, 49.38; H, 6.69; N, 8.96%. IR (KBr, $\nu_{\max}/\text{cm}^{-1}$): 3300 w (PNH), 3096 br, s (NHPh), 1626 m (Ph), 1572 s, 1502 vs ($\delta\text{S}=\text{C}=\text{NH}$), 1244 vs, 1210 m (P=O), 1018 br, vs (P–O–C). ¹H NMR (CDCl₃): δ = 1.395 (broad d, ³J_{HH} 7.0 Hz, 12H, CH₃), 4.76 (d, sept, ³J_{PH} 7.3 Hz, ³J_{HH} 6.2 Hz, 2H, OCH), 6.93 (br, d, ²J_{PH} 6.3 Hz, 1H, NHP), 7.20–7.26 (m, *p*-Ph + solvent), 7.35–7.41 (m, 2H, *m*-Ph), 7.60–7.62 (m, 2H, *o*-Ph), 10.77 (s, 1H, PhNH) ppm. ¹³C–{¹H} NMR (CDCl₃): δ = 23.61 (d, ³J_{PC} 4.9 Hz, CH₃), 23.73 (d, ³J_{PC} 4.9 Hz, CH₃), 74.05 (d, ²J_{PC} 6.6 Hz, OCH), 124.26 (s, *o*-Ph), 126.39 (s, *p*-Ph), 128.70 (s, *m*-Ph), 138.25 (s, *ipso*-Ph), 180.65 (s, C–S) ppm. $\delta^{31}\text{P}$ (CDCl₃): δ = –5.3 (q, ²J_{PH} + ³J_{PH} 6.7 Hz) ppm.

2.4. Complexes of LH with Co(II), Ni(II) and Pd(II) ions

2.4.1. General procedure

To a suspension of LH (1.2654 g, 4.0 mmol) in 30 ml of 96% ethanol, a solution of potassium hydroxide (0.2244 g, 4.0 mmol) in 30 ml of the same solvent was added, and the mixture was stirred until the ligand dissolved completely. To the resulting potassium salt of LH, a solution of M(NO₃)₂ · 6H₂O (0.6403 g for M = Co^{II}, 0.6397 g for M = Ni^{II}, 2.2 mmol, 10% excess) in 50 ml of water was

slowly added with vigorous stirring. The mixtures were kept for 5–10 h at room temperature. The resulting complexes were extracted with methylene chloride. After drying under anhydrous MgSO₄, the solvent was removed in vacuum. The residue was crystallized from a methylene chloride/*n*-hexane mixture 1:5 (v/v).

Bis-(*N*-diisopropoxyphosphinyl-*N'*-phenylthioureato-*O,S*) cobalt(II). Co[PhNHC(S)NP(O)(OPr-*i*)₂-*O,S*]₂ (**7**). Blue crystals. M.p. 117–118 °C. Yield 0.897 g, 1.30 mmol, 65%. *Anal.* Calc. for C₂₆H₄₀CoN₄O₆P₂S₂C, 45.28; H, 5.85; N, 8.12. Found C, 45.25; H, 5.70; N, 8.15%. IR (KBr, $\nu_{\max}/\text{cm}^{-1}$): 3304 (NH), 1554 s, 1522 vs (S=C=N), 1130 s (P=O), 1000 vs (P–O–C), 364 w (Co–S). EI MS *m/z*, *I*(%): 689 (M⁺, 0.11), 316 (5.50), 274 (2.00), 257 (0.44), 198 (73.10), 202 (0.50), 118 (100.00), 43 (56.74); calc. for Co[PhNHC(S)NP(O)(OPr-*i*)₂]₂: *m/z* 689.

Bis-(*N*-diisopropoxyphosphinyl-*N'*-phenylthioureato-*N,S*) nickel(II), Ni[PhNHC(S)NP(O)(OPr-*i*)₂-*N,S*]₂ (**8**). Violet crystals. M.p. 106–107 °C (dec.). Yield 1.141 g, 1.66 mmol, 83%. *Anal.* Calc. for C₂₆H₄₀N₄NiO₆P₂S₂: C, 45.30; H, 5.85; N, 8.13. Found: C, 45.36; H, 5.36; N, 7.86%. IR (KBr, $\nu_{\max}/\text{cm}^{-1}$): 3152 (NH), 1544 vs (S=C=N), 1196 s (P=O), 998 vs, broad (P–O–C), 380 w (Ni–S). EI MS *m/z*, *I*(%): 688 (M⁺, 0.04), 656.5 (0.02); 375 (2.46), 316 (26.00), 231 (25.75), 198 (69.64), 118 (89.60), 43 (100) calc. for Ni[PhNHC(S)NP(O)(OPr-*i*)₂]₂: *m/z* 688. ESI M⁺ MS, *m/z*, *I*(%): 711 (70%) [M + Na]⁺, 339 (100%) [NaL + H]⁺. ESI M[–] MS, *m/z*, *I*(%): 687 (100%) [M – H][–]. ¹H NMR (CDCl₃): δ = 1.36 (d, ³J_{HH} 6.2 Hz, 12H, CH₃), 1.66 (d, ³J_{HH} 6.2 Hz, 12H, CH₃), 4.65 (octet, ³J_{PH} + ³J_{HH} 6.6 Hz, 4H, OCH), 7.16–7.21 (m, 2H, *p*-Ph), 7.32–7.37 (m, 4H, *m*-Ph), 7.41–7.43 (m, 4H, *o*-Ph), 10.6 (s, 2H, NH) ppm. ¹³C–{¹H} NMR (CDCl₃): δ = 23.87–24.02 (m, CH₃), 72.00 (d, ²J_{P,C} = 4.8 Hz, OCH), 122.52 (s, *o*-Ph), 125.82 (s, *p*-Ph), 129.00 (s, *m*-Ph), 135.65 (s, *ipso*-Ph), 185.45 (s, C–S) ppm. ³¹P–{presup1H} NMR (CDCl₃): δ = 1.71 (s) ppm.

Bis-(*N*-diisopropoxyphosphinyl-*N'*-phenylthioureato-*N,S*) palladium(II). Pd[PhNHC(S)NP(O)(OPr-*i*)₂-*N,S*]₂ (**9**). A

Table 1
Crystal data and structure refinement for ML₂ chelates 7–9

	7	8	9
Empirical formula	C ₂₆ H ₄₀ CoN ₄ O ₆ P ₂ S ₂	C ₂₆ H ₄₀ N ₄ NiO ₆ P ₂ S ₂	C ₂₆ H ₄₀ N ₄ O ₆ P ₂ PdS ₂
<i>M</i>	689.61	689.39	737.08
Crystal system	triclinic	monoclinic	monoclinic
Space group	<i>P</i> $\bar{1}$	<i>P</i> 2 ₁ / <i>n</i>	<i>P</i> 2 ₁ / <i>n</i>
<i>a</i> (Å)	12.294(3)	10.555(2)	10.752(2)
<i>b</i> (Å)	12.427(3)	14.293(3)	14.237(3)
<i>c</i> (Å)	13.551(3)	21.741(4)	21.661(4)
α (°)	107.37(3)		
β (°)	106.94(3)	98.94(3)	98.76(3)
γ (°)	108.70(3)		
<i>V</i> (Å ³)	1691.3(11)	3240.1(11)	3277.1(11)
<i>Z</i>	2	4	4
μ (mm ^{–1})	0.768	0.871	0.835
Reflections collected/unique [<i>R</i> _{int}]	9563/5794 [0.1167]	19699/6287 [0.0606]	20722/7617 [0.0240]
Final <i>R</i> ₁ , <i>wR</i> ₂ [<i>I</i> > 2 σ (<i>I</i>)]	0.0973, 0.2342	0.0595, 0.0676	0.0280, 0.0635

thiourea LH (1.2654 g, 4.0 mmol) in 30 ml of anhydrous ethanol was converted to the potassium salt followed by Section 2.4.1 and was added dropwise with vigorous stirring to a solution of $\text{Pd}(\text{PhCN})_2\text{Cl}_2$ (0.7671 g, 2.0 mmol) in 100 ml of anhydrous ethanol. The mixtures were kept for 20 h at room temperature. The solvent was removed in vacuum. The residue was resolved in 10 ml of methylene chloride and the insoluble KCl was filtered. The product was precipitated by *n*-hexane and recrystallized from a methylene chloride/*n*-hexane mixture 1:5 (v/v). Chelate **9** forms yellow crystals. M.p. 180–182 °C. Yield 1.01 g, 1.38 mmol, 68.8%. *Anal.* Calc. for $\text{C}_{26}\text{H}_{40}\text{N}_4\text{O}_6\text{P}_2\text{PdS}_2$: C, 42.37; H, 5.47; N, 7.60. Found: C, 42.34; H, 5.36; N, 7.78%. IR (nujol, $\nu_{\text{max}}/\text{cm}^{-1}$): 3160 (NH), 1540 (S=C=N), 1200 (P=O), 1008 (P–O–C) 370, 350 (Pd–S). EI MS: M^+ not observed, calc. for $\text{Pd}[\text{PhNHC}(\text{S})\text{NP}(\text{O})(\text{OPr-}i)_2]_2$: m/z 736. ESI M^+ MS, m/z , $I(\%)$: 759 (100%) $[\text{M} + \text{Na}]^+$. ESI M^- MS, m/z , $I(\%)$: 735 (100%) $[\text{M} - \text{H}]^-$. ^1H NMR (CDCl_3): δ = 1.34 (d, $^3J_{\text{HH}}$ 6.2 Hz, 12H, CH_3), 1.50 (d, $^3J_{\text{HH}}$ 6.2 Hz, 12H, CH_3), 4.79 (d, sept, $^3J_{\text{PH}}$ 7.4 Hz, $^3J_{\text{HH}}$ 6.2 Hz, 4H, OCH), 6.89–6.92 (m, 2H, *p*-Ph), 7.00–7.05 (m, 4H, *m*-Ph), 7.44–7.47 (m, 4H, *o*-Ph), 11.58 (s, 2H, NH) ppm. ^{13}C - $\{^1\text{H}\}$ NMR (CDCl_3): δ = 23.96 (d, $^3J_{\text{PC}}$ 4.8 Hz, CH_3), 72.31 (t, $^2J_{\text{PC}}$ 5.1 Hz, OCH), 122.80 (s, *o*-Ph), 126.04 (s, *p*-Ph), 129.06 (s, *m*-Ph), 135.28 (s, *ipso*-Ph), 187.93 (s, C–S) ppm. ^{31}P - $\{^1\text{H}\}$ NMR (CDCl_3): δ = 2.69 (s) ppm.

3. Results and discussion

Chelates of Co(II) (**7**) and Ni(II) (**8**) were obtained by the reactions of $\text{M}(\text{NO}_3)_2 \cdot 6\text{H}_2\text{O}$ aqueous solutions with the potassium salt of *N*-diisopropoxyphosphinyl-*N'*-phenylthiourea (**LH**) in aqueous ethanol. The Pd(II) (**9**) complex was obtained by reacting $\text{PdCl}_2 \cdot 2\text{PhCN}$ with the potassium salt of the **LH** in ethanol. Complexes **7–9** were obtained as color crystals, stable in the air.

The obtained compounds were investigated by UV, IR, NMR ^1H , ^{13}C and ^{31}P spectroscopy, EI and ESI mass spectrometry. Intensive $[\text{ML}_2 + \text{Na}]^+$ and $[\text{ML}_2 - \text{H}]^-$ peaks were found in ESI M^+ and M^- spectra of complexes **8** and **9**. Crystal and molecular structures of complexes **7–9** were determined by single-crystal X-ray diffraction (Figs. 3 and 4). Selected bond lengths, valence and torsion angles for complexes **7**, **8**, and **9** are presented in Tables 2 and 3.

Our experiments have shown that the coordination mode of thiourea depends on the nature of the metal ion (Scheme 1). The 1,3-coordination via sulfur and phosphorylimide nitrogen atoms was found in the Ni(II) and Pd(II) complexes **8** and **9**. Phosphoryl group does not participate in the coordination in these complexes. This is the first example of the four-membered chelate ring formation in the complexes with ligands containing $\text{RC}(\text{S})\text{NHP}(\text{Y})\text{R}'_2$ unit ($\text{Y} = \text{O}, \text{S}$).

The *N,S*-coordination is not realized in the Co(II) complex **7**. Compound **7** is a spirocyclic chelate with a distorted tetrahedral CoO_2S_2 -core.

3.1. IR-spectroscopy investigations

The coordination of phosphoryl group results in the low frequencies shift when compared to the free ligand value ($\nu_{\text{as}} 1244 \text{ cm}^{-1}$). The shift of $\Delta\nu_{\text{P=O}}$ 44–48 cm^{-1} is observed for the *N,S*-coordination (**8**, **9**) and it increases up to 114 cm^{-1} in *O,S*-complexes of Co(II) (**7**). The IR spectra of thiourea **LH** clearly show the presence of the strong intramolecular $\text{PhNH} \cdots \text{O}=\text{P}$ hydrogen bonds both in the solid state and in solutions [27]. There is only one strong band in the range of 3100–3160 cm^{-1} for complexes **8** and **9** instead of two broad bands at 3300 (PNH) cm^{-1} and 3096 cm^{-1} (NHPh) in parent thiourea. The PhNH-group absorption band in complex **7** is shifted to higher frequency up to 3304 cm^{-1} due to the breaking of intramolecular $\text{PhNH} \cdots \text{O}=\text{P}$ hydrogen bonds. It is difficult to

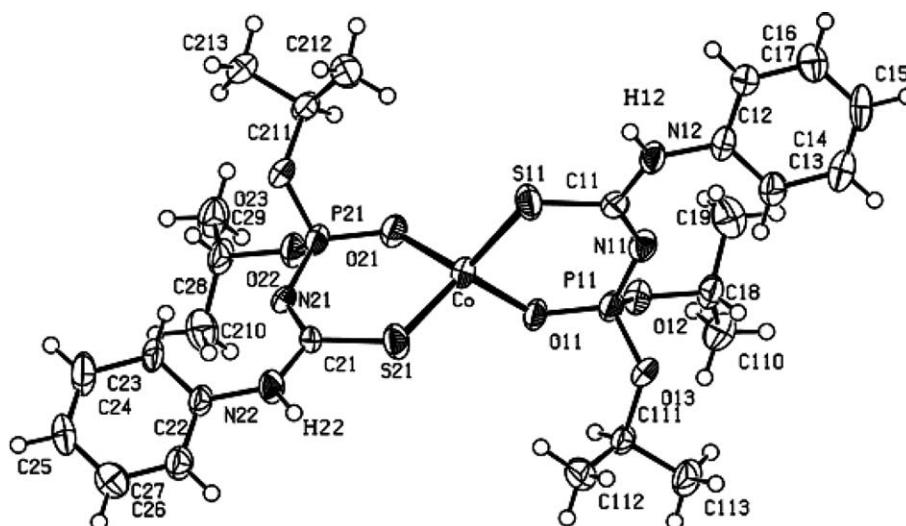


Fig. 3. Crystal structure of the complex $\text{Co}[\text{PhNHC}(\text{S})\text{NP}(\text{O})(\text{OPr-}i)_2\text{-O,S}]_2$ (**7**). The atoms are shown as 50% probability of thermal vibrations.

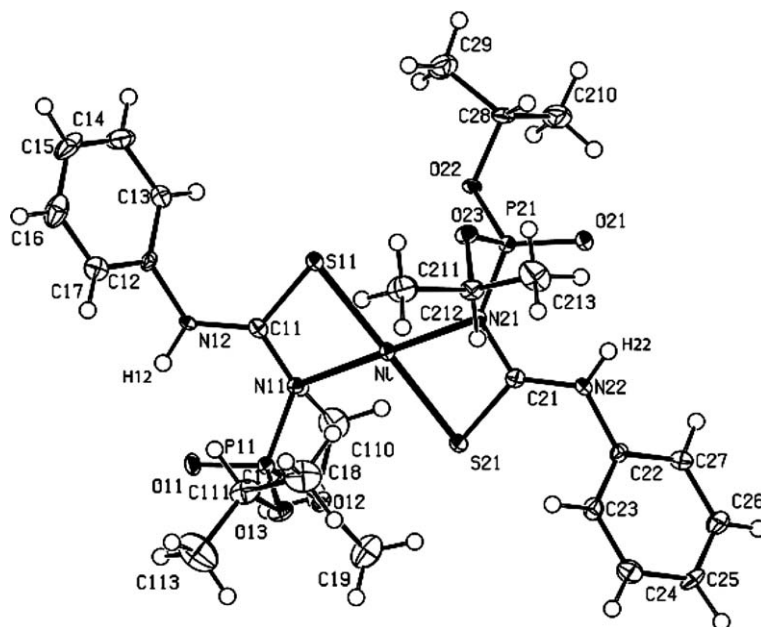


Fig. 4. Crystal structure of the complex $\text{Ni}[\text{PhNHC}(\text{S})\text{NP}(\text{O})(\text{OPr-}i)_2\text{-N,S}]_2$ (**8**). The atoms are shown as 50% probability of thermal vibrations.

Table 2
Selected bond lengths (Å), valence and torsion angles (°) for complex **7**

Co–S(11)	2.305(3)	P(11)–N(11)	1.613(7)
Co–S(21)	2.319(3)	P(21)–N(21)	1.625(7)
Co–O(11)	1.974(5)	N(11)–C(11)	1.306(10)
Co–O(21)	1.960(5)	N(21)–C(21)	1.305(11)
S(11)–C(11)	1.789(9)	N(12)–C(11)	1.358(10)
S(21)–C(21)	1.779(8)	N(22)–C(21)	1.370(10)
P(11)–O(11)	1.513(5)	N(12)–C(12)	1.428(10)
P(21)–O(21)	1.526(5)	N(22)–C(22)	1.427(9)
S(21)–Co–O(11)	119.16(17)	Co–S(11)–C(11)–N(11)	–9.0(9)
S(11)–Co–O(21)	118.25(18)	Co–S(21)–C(21)–N(21)	–8.9(9)
S(11)–Co–O(11)	99.65(16)	N(11)–P(11)–O(11)–Co	–13.9(6)
S(21)–Co–O(21)	100.03(17)	N(21)–P(21)–O(21)–Co	–14.2(6)

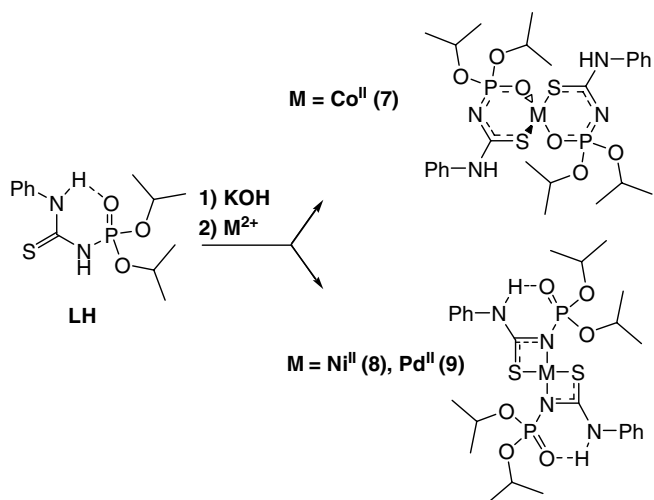
separate the specific band for the C–S and C–N groups both for thiourea **LH** and complexes **7–9**. The strong infrared absorption observed for all concerned complexes in the region $1500\text{--}1570\text{ cm}^{-1}$ was assigned to the group vibrations of the conjugated SCN fragment. The weak M–S vibration was observed at $350\text{--}380\text{ cm}^{-1}$ range.

3.2. NMR studies

Redistribution of the electronic density after deprotonation of the ligand molecules results in significant low-field shifts of the signals in ^{31}P spectra. The ^{31}P signals of complexes **8** and **9** are shifted by 6–7 ppm in comparison with

Table 3
Comparative distances (Å) and bond angles (°) computed at the PBE level with different basis sets and found from the X-ray crystal data for the $\text{M}[\text{PhNHC}(\text{S})\text{NP}(\text{O})(\text{OPr-}i)_2\text{-N,S}]_2$ complexes **8** and **9**

	8	ECP-TZVP'	TZVP'	9	ECP-TZVP'	TZVP'
M–S(11)	2.2209(13)	2.253	2.250	2.3323(8)	2.386	2.406
M–S(21)	2.2203(13)	2.253	2.250	2.3306(8)	2.386	2.406
M–N(11)	1.907(3)	1.910	1.912	2.0284(15)	2.065	2.091
M–N(21)	1.906(3)	1.910	1.912	2.0307(15)	2.065	2.091
S(11)–C(11)	1.732(4)	1.744	1.738	1.7382(19)	1.749	1.742
S(21)–C(21)	1.737(4)	1.744	1.738	1.7347(18)	1.749	1.742
N(11)–C(11)	1.332(4)	1.357	1.354	1.330(2)	1.356	1.352
N(21)–C(21)	1.342(4)	1.357	1.354	1.332(2)	1.356	1.352
N(12)–C(11)	1.337(4)	1.349	1.347	1.338(2)	1.350	1.349
N(22)–C(21)	1.329(4)	1.349	1.347	1.337(2)	1.350	1.349
P(11)–O(11)	1.471(2)	1.518	1.515	1.4664(14)	1.518	1.515
P(21)–O(21)	1.471(2)	1.518	1.515	1.4713(14)	1.518	1.515
P(11)–N(11)	1.655(3)	1.682	1.680	1.6548(16)	1.681	1.677
P(21)–N(21)	1.647(3)	1.682	1.680	1.6459(16)	1.681	1.677
N(11)–M–S(11)	74.36(9)	73.8	73.5	70.16(5)	69.1	68.4
N(21)–M–S(21)	74.50(9)	73.8	73.5	70.18(5)	69.1	68.4
O(11)–P(11)–N(11)–C(11)	21.9(4)	11.7	10.5	23.74(19)	12.4	13.8
O(21)–P(21)–N(21)–C(21)	16.6(4)	11.1	10.3	16.00(19)	12.5	13.1



Scheme 1. Coordination modes of the thiourea LH.

metal-free thiourea. The NMR signals are single narrow lines, with the line-width $\Delta\nu_{1/2}$ of 10.4 for **8** and 4.5 Hz for **9**. This strongly suggests the presence of only one complex in the solutions studied.

The NMR ^1H and ^{13}C spectra of complexes **8** and **9** also contain one set of signals.

The values of the chemical shifts and coupling constants indicate the same coordination modes in solution as it was found in the solid state.

CH_3 -proton signals in ^1H spectra of complexes **8** and **9** appear as two separate doublets with integral intensity corresponding to 24 protons. This is caused by the diastereoisomer formation upon coordination.

3.3. X-ray crystallography

3.3.1. Crystal structure of the Co^{II} complex **7**

Compound **7** is a spiro-cyclic chelate with a tetrahedral CoO_2S_2 -core (Fig. 3). Values of endocyclic $\text{S}-\text{Co}-\text{O}$ angles are reduced and exocyclic angles are increased in comparison with an ideal tetrahedron angle, 109.5° (Table 2).

The geometry of thiourea $\text{N}-\text{C}-\text{N}$ fragments shows that lone electron pairs of PhNH -group nitrogens [N(12) and N(22)] are conjugated with endocyclic $\text{N}-\text{C}$ bonds [torsion angles $\text{C}(12)\text{N}(12)\text{C}(11)\text{N}(11) - 1.9(13)^\circ$ and $\text{C}(22)\text{N}(22)\text{C}(21)\text{N}(21) - 4.3(13)^\circ$]. The endocyclic $\text{C}-\text{N}$ bonds in complex **7** are 0.052 – 0.065 Å shorter than the exocyclic ones.

At the same time, $\text{C}-\text{N}$ bond lengths (Table 2) in chelate ring are appreciably lengthened in comparison with typical $\text{C}=\text{N}$ double bond values (1.255 Å) [28], confirming the conjugation with PhNH -group nitrogen. A similar tendency is observed for the six-membered ring of *N*-thiophosphinylthiourea *S,S'*-complexes: $\text{Ni}[\text{MeNHC}(\text{S})\text{NP}(\text{S})\text{Ph}_2]_2$ [6], $\text{Ni}[\textit{n}\text{-Pr}_2\text{NC}(\text{S})\text{NP}(\text{S})(\text{OPh})_2]_2$ [7], $\text{Pt}[\text{H}_2\text{NC}(\text{S})\text{NP}(\text{S})\text{Ph}_2]_2$ (Et_2O) [2], $\text{Zn}[\text{H}_2\text{NC}(\text{S})\text{NP}(\text{S})\text{Ph}_2]_2$ [2], and $\text{Ni}[\text{PhNHC}(\text{S})\text{NP}(\text{S})(\text{OPr}^i)_2]$ (**10**). The *trans*-square-planar complex **10** is formed by thiourea $\text{PhNHC}(\text{S})\text{NHP}(\text{S})(\text{O}-\text{Pri})_2$, the nearest structure analog of the **LH** ligand. The

structure of complex **10** has been investigated by X-ray analysis [29] [bond lengths, Å: CS 1.740(3), CN_P 1.291(4), CN_Ar 1.357(4), $\text{P}-\text{N}$ 1.594(3), NiS_C 2.2073(9)].

As expected, the $\text{P}-\text{N}$ bonds in the six-membered ring of complex **7** are shortened, and $\text{P}-\text{O}$ bonds are lengthened in comparison with the data of $\text{Ni}(\text{II})$ **8** and $\text{Pd}(\text{II})$ **9** complexes (Table 3).

The CS and intracyclic CN_P bonds lengths in the *S,S'*-chelate **10** are noticeably shorter than in complex **7** (Table 2). The $\text{P}-\text{N}$ bonds in **7** are longer than those in the chelate **10**. It suggests the lower degree of negative charge delocalization in the chelate ring of **7**.

The six-membered ring $\text{M}-\text{S}^1-\text{P}-\text{N}-\text{C}-\text{S}^2$ in the complexes of *N*-thioacylamidophosphinates $\text{RC}(\text{S}^1)\text{NHP}(\text{S}^2)\text{R}'_2$ usually has a distorted boat conformation [2,6,7,9,29]. On the contrary, the chelate rings in **7** are significantly flattened (Table 2).

The hydrogen bonds in the crystal of complex **7** were not found.

3.3.2. Crystal structures of the Ni^{II} and Pd^{II} complexes **8** and **9**

The metal center in **8** and **9** has a distorted square-planar MN_2S_2 environment with *trans*-configuration of ligands. Sums of valence angles around nickel and palladium atoms in complexes **8** and **9** are close to 360° . Endocyclic $\text{S}-\text{M}-\text{N}$ angles are more than 30° smaller than the exocyclic ones (Table 3).

Thus, $\text{S}-\text{M}-\text{N}$ intracyclic angles ($\text{M} = \text{Ni}^{\text{II}}, \text{Pd}^{\text{II}}$) in four-membered cycles do not exceed 70 – 78° in contrast with $\text{O}-\text{Co}-\text{S}$ angles in six-membered chelate ring of **7** (Table 2).

The formation of a six-membered chelate ring in the tetrahedral complex **7** is more tolerable by steric reasons. Steric requirements of *N,S*-chelates can make a strong distortion of tetrahedral complex core. The average distances between N_P and S donor centers are only 2.51 Å for complex **8** and 2.52 Å for complex **9**. The average $\text{O}-\text{S}$ distance in *1,5-O,S*-complex **7** is 3.28 Å. It is obvious that significant distortion of tetrahedral metal geometry would require to achieve similar distance in the case of *1,3-N,S*-coordination to Co^{II} cation.

The $\text{C}-\text{S}$ bond lengths are shorter, while the CN_P bond lengths in the four-membered rings **8** and **9** (Table 3) are longer than those in the six-membered *O,S*-chelate of **7** (Table 2) and *S,S'*-chelate of **10**. The $\text{P}-\text{N}$ bonds in complexes **8** and **9** are single and $\text{P}=\text{O}$ bonds are double according to their bond lengths [30].

The one of the exocyclic carbon–nitrogen bond $\text{N}(22)-\text{C}(21)$ in complex **8** is slightly shorter than the endocyclic $\text{N}(21)-\text{C}(21)$ by 0.013 Å. In all the other cases, $\text{C}-\text{N}$ bond lengths in the thiourea group in complexes **8** and **9** are practically identical (Table 3). Their values agree well with the average values of the thiourea CN bond lengths in complex **7** (1.3348 Å). The $\text{C}-\text{N}$ bonds lengths in thiourea fragments of **8** and **9** (in comparison with complex **7**) indicate the strengthening of conjugation between the electronic pairs of $\text{N}(12)$ and $\text{N}(22)$ and intracyclic $\text{C}-\text{N}$ bonds.

In both cases, the N–C–N–P–O moiety exhibits *syn,syn* conformation because of H-bonding. The PhNH groups are bonded by two weak H-bonds of NH–O=P type: first is the intramolecular bond and the second one is of the intermolecular type involving P=O group of the neighboring molecule (Fig. 5, Table 4). Molecules of the chelates **8** and **9** in the crystals form the infinite planar rows along the *a0c* plane.

3.4. Theoretical calculations of Ni(II) and Pd(II) complexes with the PhNHC(S)NHP(O)(OPr-*i*)₂ ligand

Quantum-chemical calculations have been performed for vacuum using the density functional theory (DFT) method within the generalized gradient approximation (GGA) [31] for the exchange-correlation functional of Perdew, Burke and Ernzerhof (PBE) [32] as implemented in an original program package “Priroda” developed by D.N. Laikov [33]. We used 311-split basis set for main group elements with one additional polarization p-function for hydrogen and two additional polarization d-functions for other elements, referred to as TZVP'. At the first stage, the fully unconstrained geometry optimization has been carried out with relativistic Stevens–Basch–Krauss (SBK) effective core potentials (ECP) [34] optimized for DFT-

calculations. After that, all the calculations were refined using all-electron basis set. In order to characterize the nature of the obtained stationary points (minima or saddle points), the analytical calculations of the second derivatives of energy with respect to coordinate (Hessian matrix) have been performed. For all investigated species, a frequency analysis has been carried out. All minima have been checked for the absence of imaginary frequencies. Energies of the lower-lying excited (singlet) states at the optimal geometry were computed by single-point time-dependent density functional theory (TD-DFT) calculation with the PBE functional and the TZVP' basis set.

Originally, the geometry of the possible isomers, *trans*-M[PhNHC(S)NP(O)(OPr-*i*)₂-O,S]₂, *cis*-M[PhNHC(S)NP(O)(OPr-*i*)₂-O,S]₂, and *trans*-M[PhNHC(S)NP(O)(OPr-*i*)₂-N,S]₂ (M^{II} = Ni^{II}, Pd^{II}), has been optimized. The values of the optimized structure energies in the TZVP' basis (*E*) were found to be –4670.780196, –4670.781331, and –4670.802593 a.u. (Hartree), respectively, for *trans*-Ni[PhNHC(S)NP(O)(OPr-*i*)₂-O,S]₂, *cis*-Ni[PhNHC(S)NP(O)(OPr-*i*)₂-O,S]₂, and *trans*-Ni[PhNHC(S)NP(O)(OPr-*i*)₂-N,S]₂ as well as –8102.408273, –8102.411100, and –8102.433021 a.u., respectively, for *trans*-Pd[PhNHC(S)NP(O)(OPr-*i*)₂-O,S]₂, *cis*-Pd[PhNHC(S)NP(O)(OPr-*i*)₂-O,S]₂, and *trans*-Pd[PhNHC(S)NP(O)(OPr-*i*)₂-N,S]₂. Thus,

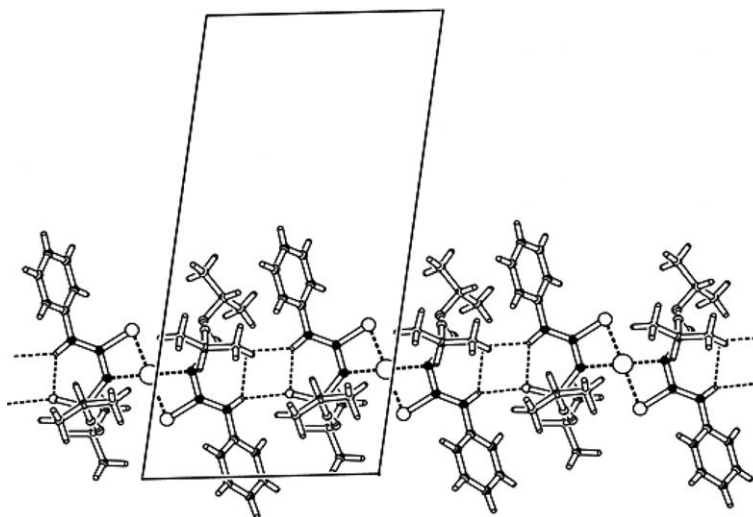


Fig. 5. Structure of H-bonded chains in the crystal of Ni[L-N,S]₂ complex **8**.

Table 4
Parameters of hydrogen bonds for **8** and **9** (distances, *d* (Å), and angles (°))

D–H···A	N(12)–H(12)···O(11) intramolecular		N(12)–H(12)···O(21) ^a		N(22)–H(22)···O(21) intramolecular		N(22)–H(22)···O(11) ^a	
	8	9	8	9	8	9	8	9
<i>d</i> (D–H)	0.93(4)	0.77(2)	0.93(4)	0.77(2)	0.83(3)	0.80(3)	0.83(3)	0.79(2)
<i>d</i> (H···A)	2.16(4)	2.29(2)	2.07(4)	2.17(2)	2.22(3)	2.22(3)	2.21(3)	2.25(2)
<i>d</i> (D···A)	2.876(4)	2.906(2)	2.856(4)	2.824(2)	2.854(4)	2.866(2)	2.945(4)	2.913(2)
∠(DHA)	134(3)	137(2)	142(3)	144(2)	133(3)	139(2)	148(3)	142(2)
∠A···H···A ^a	83.3(13)	78.4(7)			78.7(11)	78.4(8)		
∑ _H	359(4)	359(3)			360(4)	359(3)		

^a Neighbor molecule.

the optimized forms *trans*-Ni[PhNHC(S)NP(O)(OP*r*-*i*)₂-*N,S*]₂ and *trans*-Pd[PhNHC(S)NP(O)(OP*r*-*i*)₂-*N,S*]₂ are most stable among the above-mentioned isomers of the Ni(II) and Pd(II) complexes in agreement with the experimental data obtained for **8** and **9**. As can be seen from Table 3, the distances and bond angles computed and found by X-ray for both *trans*-Ni[PhNHC(S)NP(O)(OP*r*-*i*)₂-*N,S*]₂ and *trans*-Pd[PhNHC(S)NP(O)(OP*r*-*i*)₂-*N,S*]₂ are close to each other. Moreover, use of the ECP basis set results in very quick convergence to the similar if not better values than all-electron basis set. As expected, an agreement between the calculated and X-ray data for Ni(II) complex is much better than that for the Pd(II) complex.

The calculated O11–H12 and O21–H22 distances are markedly shorter than those found experimentally in the crystals and this may result from the fact that in isolated complex molecule there are strong intramolecular hydrogen bonds, while there are weak intramolecular and intermolecular H-bonds of NH···O=P type in the crystals (Fig. 6A). We have made the estimation of energetic contribution of two intramolecular NH···O=P hydrogen bonds by the following computation experiment (basis TZVP' with ECP). Increasing two torsion angles for the energetically favorable forms C11–N11–P11–O11 and C21–N21–P21–O21 (Table 3) up to 60° (Fig. 6B) and constraining these values for geometry optimization caused loss of 57.3 and 52.9 kJ/mol energy, respectively, for *trans*-Ni[PhNHC(S)NP(O)(OP*r*-*i*)₂-*N,S*]₂ and *trans*-Pd[PhNHC(S)NP(O)(OP*r*-*i*)₂-*N,S*]₂. Such assumption brings to the most possible lengthening of two intramolecular

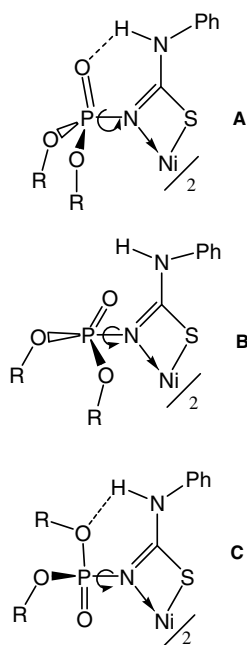


Fig. 6. Intramolecular NH···O hydrogen bonds in *trans*-M[PhNHC(S)NP(O)(OP*r*-*i*)₂-*N,S*]₂ (M = Ni(II); Pd(II)) complexes: (A) NH···O=P hydrogen bonds in crystal structure, (B) breaking of hydrogen bonds by increasing the C–N–P=O torsion angles up to 60° (used in DFT calculation), (C) NH···(OP*r*-*i*)P bonds.

NH···O=P bonds. Hence, the estimated energy of the hydrogen bonds is at least 25 kJ/mol (per each bond) as demonstrated by our computational experiment. Further increasing of the torsion angle values results in the local minimum of energy due to the formation of two very weak NH···(OP*r*-*i*)P bonds (Fig. 6C) instead of NH···O=P bonds.

The calculated energies of the four most intensive singlet-singlet d–d electronic transitions are 15360 cm⁻¹ (λ_{\max} 651.0 nm), 17880 cm⁻¹ (λ_{\max} 559.3 nm), 18960 cm⁻¹ (λ_{\max} 527.4 nm), and 20330 cm⁻¹ (λ_{\max} 491.9 nm) for Ni[PhNHC(S)NP(O)(OR)₂-*N,S*]₂ as well as 18492 cm⁻¹ (λ_{\max} 540.8 nm), 20840 cm⁻¹ (λ_{\max} 479.9 nm), 23580 cm⁻¹ (λ_{\max} 424.1 nm), and 25440 cm⁻¹ (λ_{\max} 393.1 nm) for Pd[PhNHC(S)NP(O)(OR)₂-*N,S*]₂. In the experimental electronic absorption spectra of the complex solutions (Fig. 7), two bands at 615 and 487 nm for Ni[PhNHC(S)NP(O)(OP*r*-*i*)₂-*N,S*]₂ and two “shoulders” at ~440 and ~390 nm for Pd[PhNHC(S)NP(O)(OP*r*-*i*)₂-*N,S*]₂ are observed. High-energy transition in each case can be assigned to the calculated one, but some of the calculated transitions have small intensities and are practically unobserved. Early [35,36] three bands in the absorption spectra of Ni[S₂CNET₂-*S,S'*]₂ (at 15900, 19000, and 21000 cm⁻¹) [35] and Ni[PhC(S)NP(S)(OP*r*-*i*)₂-*S,S'*]₂ (at 16530, 18920, and 21960 cm⁻¹) [36] were assigned, respectively, to the transitions ¹A_{1g} → ¹B_{1g} (d_{x²-y²} → d_{xy}), ¹A_{1g} → ¹B_{3g} (d_{xz} → d_{xy}), and ¹A_{1g} → ¹B_{1g} (d_{z²} → d_{xy}) for the local D_{2h} symmetry. Thus, the calculated energies 15360, 17880, and 20330 cm⁻¹ for Ni[PhNHC(S)NP(O)(OP*r*-*i*)₂-*N,S*]₂ with the same D_{2h} symmetry can be related to the ¹A_{1g} → ¹B_{1g} (d_{x²-y²} → d_{xy}), ¹A_{1g} → ¹B_{3g} (d_{xz} → d_{xy}), and ¹A_{1g} → ¹B_{1g} (d_{z²} → d_{xy}) transitions, respectively. Similar assignment is suitable for the analogous Pd(II) complex **9** (see, for example, Ref. [37]). The above spectral data indicate rather strong crystal field splitting (10 Dq) in the M[PhNHC(S)NP(O)(OP*r*-*i*)₂-*N,S*]₂ complexes because energy of the ¹A_{1g} → ¹B_{1g} (d_{x²-y²} → d_{xy}) transition is equal

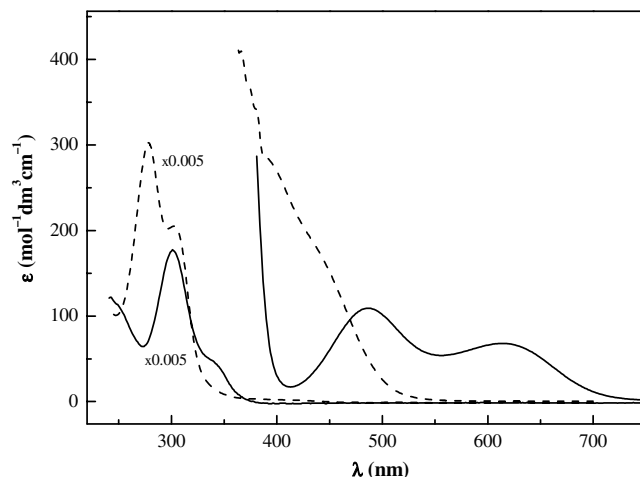


Fig. 7. Electronic absorption spectra of the complexes Ni[L-*N,S*]₂ (**8**) (solid line) and Pd[L-*N,S*]₂ (**9**) (dashed line) in CH₂Cl₂.

to 10 $Dq-C$ (C is an interelectronic repulsion Racah parameter) [37]. The estimated 10 Dq values for the complexes $M[\text{PhNHC(S)NP(O)(OPr-}i\text{)}_2\text{-}N,S\text{]}_2$ ($M^{\text{II}} = \text{Ni}^{\text{II}}, \text{Pd}^{\text{II}}$) are close to those observed for the $\text{Ni}^{\text{II}}\text{S}_4$ and $\text{Pd}^{\text{II}}\text{S}_4$ cores [37].

This provides the higher crystal field stabilization energies (CFSE) for the $\text{Ni}[\text{PhNHC(S)NP(O)(OPr-}i\text{)}_2\text{-}N,S\text{]}_2$ isomer and particularly $\text{Pd}[\text{PhNHC(S)NP(O)(OPr-}i\text{)}_2\text{-}N,S\text{]}_2$ isomer with low-spin d^8 configuration in comparison to the corresponding $M[\text{PhNHC(S)NP(O)(OPr-}i\text{)}_2\text{-}O,S\text{]}_2$ species containing coordinated oxygen donor atoms.

4. Conclusion

According to the discussion presented above, there are two reasons for the higher stability of the $M[\text{PhNHC(S)NP(O)(OPr-}i\text{)}_2\text{-}N,S\text{]}_2$ isomers relatively to $M[\text{PhNHC(S)NP(O)(OPr-}i\text{)}_2\text{-}O,S\text{]}_2$ isomers ($M^{\text{II}} = \text{Ni}^{\text{II}}, \text{Pd}^{\text{II}}$). One of the reasons is the formation of intramolecular $\text{NH}\cdots\text{O}=\text{P}$ hydrogen bonds. The other reason derives from the deprotonated NH group of $\text{PhNHC(S)NP(O)(OPr-}i\text{)}_2\text{-}N,S\text{]}_2$, which is a powerful electron donor comparable to the deprotonated peptide bond nitrogen [38]. Stronger ligand field is caused by the amide $\text{N}^{(-)}$ atom when compared to the oxygen atom of $\text{P}=\text{O}$ group. This determines higher crystal field stabilization energies (CFSE) for the low-spin d^8 $M[\text{PhNHC(S)NP(O)(OPr-}i\text{)}_2\text{-}N,S\text{]}_2$.

In the case of the $\text{Co}[\text{PhNHC(S)NP(O)(OPr-}i\text{)}_2\text{-}O,S\text{]}_2$ complex, the 1,5- O,S -coordination is realized for two reasons: (i) as mentioned above, the steric hindrances associated with strong distortion of tetrahedral environment of central ion inhibit the formation of 1,3- N,S -chelate; (ii) CFSE for d^7 configuration (Co^{II}) is much lower than that for the low-spin d^8 configuration ($\text{Ni}^{\text{II}}, \text{Pd}^{\text{II}}$).

Thus, the structure of N -thioacylamidophosphinate (**2**) complexes with Ni^{II} and Pd^{II} strongly depends on the nature of the substituents at $-\text{C(S)NHP(O)}<$ fragment. An electron withdrawing effect of phenyl at the thioamide ligand HQ and the absence of intramolecular hydrogen bonds prevent the 1,3- N,S chelate formation in this case [12,16].

Acknowledgements

This work was supported by the Russian Foundation for Basic Research (Grant Nos. 03-03-32372-a, 03-03-96225-r2003tatarstan_a), the joint program of CRDF and the Russian Ministry of Education (BHRE 2004 Y2-C-07-02), and grant of the Russian Ministry of Education SPGA (Code A03-2.9-562). Felix Sokolov thanks Faculty of Chemistry of University of Wroclaw for scholarship.

Appendix A. Supplementary data

Supplementary data associated with this article can be found, in the online version, at [doi:10.1016/j.ica.2006.01.014](https://doi.org/10.1016/j.ica.2006.01.014).

References

- [1] (a) N.G. Zabiroy, F.M. Shamsevaleev, R.A. Cherkasov, *Uspekhi Khimii* 60 (10) (1991) 2189; (b) R.M. Kamalov, M.G. Zimin, A.N. Pudovic, *Uspekhi Khimii* 54 (12) (1985) 2044; (c) T.Q. Ly, J.D. Woollins, *Coord. Chem. Rev.* 176 (1998) 451.
- [2] D.J. Birdsall, J. Green, T.Q. Ly, J. Novosad, M. Necas, A.M.Z. Slawin, J.D. Woollins, Z. Zak, *Eur. J. Inorg. Chem.* 9 (1999) 1445.
- [3] C. Silvestru, J.E. Drake, *Coord. Chem. Rev.* 223 (2001) 117.
- [4] N.G. Zabiroy, V.V. Brus'ko, S.V. Kashevarov, F.D. Sokolov, V.A. Shcherbakova, A.Yu. Verat, R.A. Cherkasov, *Russ. J. Gen. Chem.* 8 (2000) 1214.
- [5] N.G. Zabiroy, F.M. Shamsevaleev, R.A. Cherkasov, *Russ. J. Gen. Chem.* 60 (3) (1990) 464.
- [6] T. Iwamoto, F. Ebina, H. Nakazawa, C. Nakatsuka, *Bull. Chem. Soc. Jpn.* 52 (1979) 1857.
- [7] Z. Zak, T. Gloviak, N.T.T. Chau, E.Z. Herrmann, *Anorg. Allg. Chem.* 586 (7) (1990) 136.
- [8] V.V. Brusko, A.I. Rakhmatullin, N.G. Zabiroy, *Russ. J. Gen. Chem.* 10 (2000) 1603.
- [9] N.G. Zabiroy, I.A. Litvinov, O.N. Kataeva, S.V. Kashevarov, F.D. Sokolov, R.A. Cherkasov, *Russ. J. Gen. Chem.* 9 (1998) 1408.
- [10] N.G. Zabiroy, V.N. Solov'ev, F.M. Shamsevaleev, R.A. Cherkasov, I.V. Martynov, *Russ. J. Gen. Chem.* 8 (1991) 1608.
- [11] (a) K.R. Koch, C. Sacht, S. Bourne, *Inorg. Chim. Acta* 232 (1995) 109; (b) R.A. Barley, K.I. Rothaupt, R.A. Kulling, *Inorg. Chim. Acta* 147 (1988) 233; (c) A. Irving, K.R. Koch, M.C. Matoetoe, *Inorg. Chim. Acta* 206 (1993) 193; (d) K.R. Koch, M.C. Matoetoe, *Magn. Reson. Chem.* 29 (1991) 1158; (e) V.G. Fitzl, L. Beyer, J. Sieler, R. Richter, J. Kaiser, E. Hoyer, *Z. Anorg. Allg. Chem.* 433 (1977) 237; (f) K.R. Koch, J. Toit, M.R. Cairns, C. Sacht, *J. Chem. Soc., Dalton Trans.* 5 (1994) 785; (g) K.R. Koch, C. Sacht, T. Grimmbacher, S. Bourne, *S. Afr. J. Chem.* 48 (1/2) (1994) 71.
- [12] F.D. Sokolov, N.G. Zabiroy, A.Yu. Verat, L.N. Yamalieva, D.B. Krivolapov, I.A. Litvinov (in preparation).
- [13] A.L. Konkin, V.G. Shtyrlin, N.G. Zabiroy, A.V. Aganov, L.E. Zapechelnuk, S.V. Kashevarov, A.V. Zakharov, *Russ. J. Inorg. Chem.* 41 (7) (1996) 1107.
- [14] N.G. Zabiroy, V.N. Solov'ev, F.M. Shamsevaleev, R.A. Cherkasov, A.N. Chekhlov, A.G. Tsyfarkin, I.V. Martynov, *J. Gen. Chem. USSR* 3.2 (1991) 597.
- [15] F.D. Sokolov, D.A. Safin, N.G. Zabiroy, L.N. Yamalieva, D.B. Krivolapov, I.A. Litvinov, *Mendeleev Commun.* 14 (2) (2004) 51.
- [16] B.I. Khairutdinov, V.G. Shtyrlin, A.Yu. Verat, F.D. Sokolov, N.G. Zabiroy, L.N. Yamalieva, V.V. Klochkov, *Coll. Articles "Structure and Dynamics of Molecular Systems" (Yalchik-2002)*, Moscow-Kazan-Yoshkar-Ola, 2003, N.10, part. 3, p. 269.
- [17] A.M.Z. Slawin, M.B. Smith, J.D. Woollins, *Polyhedron* 17 (25) (1998) 4465.
- [18] A. Silvestru, D. Bilc, R. Rosler, J.E. Drake, I. Haiduc, *Inorg. Chim. Acta* 305 (2000) 106.
- [19] P.Z. Zak, M. Fofana, J. Kamenicek, T. Glowiak, *Acta. Crystallogr., Sect. C* 45 (1989) 1686.
- [20] M. Necas, M.R.S.J. Foreman, J.J. Marek, J.D. Woollins, J. Novosad, *New J. Chem.* 25 (2001) 1256.
- [21] P. Bhattacharyya, A.M.Z. Slawin, J.D. Woollins, *J. Chem. Soc., Dalton Trans.* 10 (2000) 1545.
- [22] K.R. Koch, *Coord. Chem. Rev.* 216–217 (2001) 473.
- [23] G.M. Sheldrick, *SHELXS-97*, Program for Crystal Structure Solutions, University of Göttingen, Germany, 1997.

- [24] G.M. Sheldrick, SHELXL-97, Program for Crystal Structure Refinement, University of Göttingen, Germany, 1997.
- [25] A.L. Spek, *Acta Crystallogr.* 46 (1) (1990) 34.
- [26] E.S. Levchenko, I.N. Ghmurova, *Ukrainsky khimichesky zhurnal* 22 (5) (1956) 623.
- [27] R.G. Islamov, M.G. Zimin, R.M. Kamalov, I.S. Pominov, A.N. Pudovic, *Zh. Obshch. Khim.* 53 (12) (1983) 2659.
- [28] E. Bayer, G. Hefelinger, *Chem. Ber.* 99 (5) (1966) 1689.
- [29] V.V. Brusko, A.I. Rakhmatullin, V.G. Shtyrlin, D.B. Krivolapov, I.A. Litvinov, N.G. Zabiroy, *Polyhedron* (in press).
- [30] F.H. Allen, O. Kennard, D.G. Watson, L. Brammer, A.G. Orpen, R.J. Taylor, *Chem. Soc., Perkin Trans. II* 12 (1987) S1.
- [31] R.G. Parr, W. Yang, *Density-Functional Theory of Atoms and Molecules*, Oxford University Press, Oxford, 1989.
- [32] J.P. Perdew, K. Burke, M. Ernzerhof, *Phys. Rev. Lett.* 77 (1996) 3865.
- [33] (a) D.N. Laikov, *Chem. Phys. Lett.* 281 (1997) 151;
(b) Yu.A. Ustynyuk, L.Yu. Ustynyuk, D.N. Laikov, V.V. Lunin, *J. Organomet. Chem.* 597 (2000) 182.
- [34] (a) W.J. Stevens, H. Basch, M. Krauss, *J. Chem. Phys.* 81 (1984) 6026;
(b) W.J. Stevens, H. Basch, M. Krauss, P. Jasien, *Can. J. Chem.* 70 (1992) 612;
(c) T.R. Cundari, W.J. Stevens, *J. Chem. Phys.* 98 (1993) 5555.
- [35] R.H. Dingle, *Inorg. Chem.* 10 (1971) 1141.
- [36] V.V. Brusko, A.I. Rakhmatullin, V.G. Shtyrlin, N.G. Zabiroy, *Russ. J. Gen. Chem.* 70 (2000) 1521.
- [37] A.B.P. Lever, *Inorganic Electronic Spectroscopy*, 2nd ed., Elsevier, Amsterdam, 1984.
- [38] V.G. Shtyrlin, E.L. Gogolashvili, A.V. Zakharov, *J. Chem. Soc., Dalton Trans.* (1989) 1293.